SCI. MAR., 69 (Suppl. 1): 85-96 SCIENTIA MARINA 2005

PROMOTING MARINE SCIENCE: CONTRIBUTIONS TO CELEBRATE THE 50TH ANNIVERSARY OF *SCIENTIA MARINA*.
C. MARRASÉ and P. ABELLÓ (eds.)

Anthropogenic CO_2 in the ocean

TSUNG-HUNG PENG

NOAA/AOML, 4301 Rickenbacker Causeway, Miami, FL 33149, USA. E-mail: Tsung-Hung.Peng@noaa.gov

SUMMARY: The focus of this review article is on the anthropogenic CO_2 taken up by the ocean. There are several methods of identifying the anthropogenic CO_2 signal and quantifying its inventory in the ocean. The ΔC^* method is most frequently used to estimate the global distribution of anthropogenic CO_2 in the ocean. Results based on analysis of the dataset obtained from the comprehensive surveys of inorganic carbon distribution in the world oceans in the 1990s are given. These surveys were jointly conducted during the World Ocean Circulation Experiment (WOCE) and the Joint Global Ocean Flux Study (JGOFS). This data set consists of 9618 hydrographic stations from a total of 95 cruises, which represents the most accurate and comprehensive view of the distribution of inorganic carbon in the global ocean available today. The increase of anthropogenic CO_2 in the ocean during the past few decades is also evaluated using direct comparison of results from repeat surveys and using statistical method of Multi-parameter Linear Regression (MLR). The impact of increasing oceanic anthropogenic CO_2 on the calcium carbonate system in the ocean is reviewed briefly as well. Extensive studies of $CaCO_3$ dissolution as a result of increasing anthropogenic CO_2 in the ocean have revealed several distinct oceanic regions where the $CaCO_3$ undersaturation zone has expanded.

Keywords: anthropogenic carbon, distribution in ocean, chemistry impact.

RESUMEN: CO_2 ANTROPOGÉNICO EN EL OCÉANO. – El objetivo de este artículo de revisión se basa en el CO_2 de origen antropogénico que capta el océano. Hay diversos métodos para identificar la señal del CO_2 antropogénico y cuantificar su registro en el océano. El método de ΔC^* es el que se utiliza mas frecuentemente para estimar la distribución global del CO_2 antropogénico en el océano. Los resultados que se muestran se derivan de análisis realizados sobre datos de los años 1990 obtenidos a partir de estudios muy completos de distribución de carbono inorgánico en los océanos del mundo. Estos estudios fueron realizados durante el "World Ocean Circulation Experiment (WOCE)" y el "Joint Global Ocean Flux Study (JGOFS)". La base de datos incluye 9618 estaciones hidrográficas de un total de 95 campañas oceanográficas, las cuales representan la visión mas precisa y completa de la distribución global del carbono inorgánico disponible hoy en día en los océanos. El incremento del CO_2 antropogénico en el océano durante las últimas décadas es también evaluado utilizando comparaciones directas de los resultados de reiteradas investigaciones y utilizando métodos estadísticos de regresión lineal multiparamétrica (MLR). El impacto del creciente del CO_2 antropogénico sobre el carbonato cálcico de los océanos también es brevemente revisado. Un amplio número de estudios sobre la disolución del $CaCO_3$ como resultado del incremento del CO_2 antropogénico en el océano han revelado distintas regiones oceánicas donde las zonas con baja saturación de $CaCO_3$ se han expandido.

Palabras clave: carbono antropogénico, distribución en el océano, impacto químico.

INTRODUCTION

The atmospheric CO_2 concentration is considered as one of the key factors affecting the climate change because of its greenhouse warming effect. In the recent past glacial-interglacial period, the atmospheric CO_2 changed from 200 parts per million (ppm) about 18,000 years ago to 280 ppm about 11,000 years ago (Neftel *et al*., 1994). Since the industrial revolution in the early 18th century, the atmospheric CO_2 concentration has continued to rise mainly as a result of fossil fuel burning and land use activities. As of today, the atmospheric CO_2 concentration is approaching 380 ppm (Keeling and Whorf, 1994). Such a high increase of CO_2 concentration in the atmosphere in a short time has a critical implication

regarding the future climate change. The important question to ask is how the anthropogenic carbon distributes in atmosphere-ocean-earth system once it is emitted into the atmosphere. The current understanding is that about 50% of the CO_2 released by human activities has remained in the atmosphere, and the rest is taken up by the ocean and terrestrial biosphere (Sabine *et al.,* 2004). In this review article, the focus is on the anthropogenic CO_2 taken up by the ocean.

ESTIMATING ANTHROPOGENIC CO_2 INVENTORY IN THE OCEAN

There are several methods of identifying the anthropogenic CO_2 signal and quantifying its inventory in the ocean. The first method of yielding the total specific anthropogenic inventory from a regional ocean CO_2 survey results is the computation of excess CO_2 reported separately by Brewer (1978) and Chen and Millero (1979). They suggested that the anthropogenic CO_2 in the interior of ocean can be estimated by two steps: (1) determine a so-called preformed concentration of total dissolved inorganic carbon (DIC) by making corrections to the measured concentration of the DIC by subtracting the amount incurred due to the remineralization of organic matter and the dissolution of carbonates since the water sample lost contact with the surface, and (2) subtracting the pre-industrial DIC as determined from the preformed concentration in deep water, believed to be uncontaminated with anthropogenic CO_2 from the corrected DIC in step 1. This pioneering approach was not accepted widely because of the large uncertainties associated with the estimates of preformed DIC contents for different water masses in the pre-industrial era, inadequate treatments for the effect of mixing of different water types [*Shiller*, 1981], and uncertainties in the use of constant stoichiometric ratios and of the apparent oxygen utilization (AOU) for estimating the input of CO_2 from the oxidation of organic matter (Shiller, 1981; Shiller 1982; Broecker *et al.,* 1985). Gruber *et al.* (1996) developed a new method on the basis of this approach, with special attention to eliminate factors that caused possible biases. The basic equations of this method can be expressed as follows:

$$C_{ant}\ (\mu mol/kg) = C_m - \Delta C_{bio} - C_{280} - \Delta C_{dis} \qquad (1)$$

where C_{ant} is the anthropogenic CO_2 concentration in μmol/kg; C_m is the measured DIC; ΔC_{bio} is the change in DIC as a result of biological activity; C_{280} is the DIC in equilibrium with an atmospheric pCO_2 of 280 μatm; and ΔC_{dis} is the difference in DIC as a result of air-sea difference in pCO_2

This method employs a new quasi-conservative tracer ΔC^*, which is defined as the difference between the measured DIC, corrected for biological effects, and the DIC these waters would have at the surface in equilibrium with atmospheric pCO_2 of pre-industrial time:

$$\Delta C^* = C_m - \Delta C_{bio} - C_{280} \qquad (2)$$

Re-arranging Equation (1) we have:

$$\Delta C^* = C_{ant} + \Delta C_{dis} \qquad (3)$$

Hence, ΔC^* represents both the anthropogenic CO_2 and the air-sea CO_2 disequilibrium. The second term ΔC_{dis} can be determined using either information about the water age (derived from transient tracers such as CFCs or ^3H-^3He) or the distribution of ΔC^* in regions free of anthropogenic transient. The ΔC_{bio} in Equation (2) can be estimated by:

$$\Delta C_{bio} = R_C\,(O_2 - O_2^{sat}) + 0.5\,(Alk - Alk^o + R_N\,(O_2 - O_2^{sat}))$$

where R_C is the remineralization ratio C:O_2 and R_N is the remineralization ratio N:O_2 (for example, using results from Anderson and Sarmiento, 1994). The preformed alkalinity (Alk^o) of a subsurface water sample is an estimate of the alkalinity that the water has when it was last at the surface. This value is necessary not only to estimate the ΔC_{bio} but also to determine the equilibrium DIC of the waters (C_{280} is calculated using salinity, temperature, Alk^o, and pCO_2 of 280 μatm). The proper estimates of Alk^o and ΔC_{dis} are crucial in obtaining reliable estimates of C_{ant}. There are a number of modifications on the techniques of estimating these values (details given in the Indian Ocean, Sabine *et al.*, 1999; in the Pacific Ocean, Sabine *et al.*, 2002; and in the Atlantic Ocean, Perez *et al.*, 2002, and Lee *et al.*, 2003) since the initial approach of Gruber *et al.* (1996). These modifications result in improvement of the uncertainty in estimating the anthropogenic CO_2 in the ocean.

A global synthesis of anthropogenic CO_2 in the ocean has been reported recently (Sabine *et al.*, 2004). The database used for the analysis comes from a comprehensive survey of inorganic carbon distributions in the global ocean in the 1990s. These

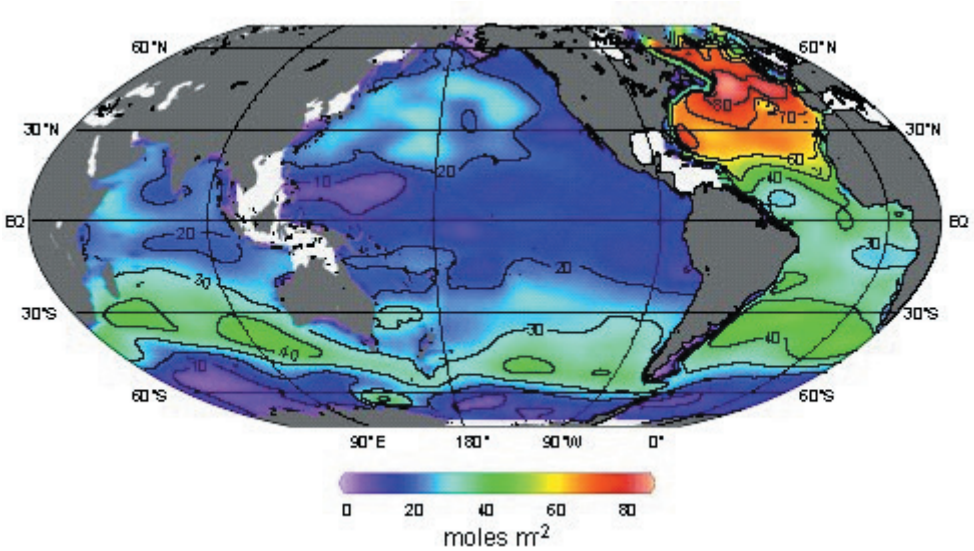

FIG. 1. – Column inventory of anthropogenic CO_2 in the ocean (mol m^{-2}). Total inventory of shaded regions is 106 ± 17 pg C. (Sabine *et al.*, 2004)

surveys were jointly conducted during the World Ocean Circulation Experiment (WOCE) and the Joint Global Ocean Flux Study (JGOFS). This data set consists of 9618 hydrographic stations from a total of 95 cruises, which represents the most accurate and comprehensive view of the distribution of inorganic carbon in the global ocean available today. Using the ΔC* method to separate the anthropogenic CO_2 from the measured DIC, the anthropogenic CO_2 signal has been determined separately in the three individual oceans (Sabine *et al.*, 1999 and 2002; Lee *et al.*, 2003). Sabine *et al.* (2004) synthesized these individual ocean estimates and provided an ocean data-constrained global estimate of cumulative oceanic sink for anthropogenic CO_2 for the period from ~1800 to 1994.

DISTRIBUTION AND INVENTORIES OF ANTHROPOGENIC CO_2 IN THE OCEAN

To generate a global anthropogenic CO_2 inventory, the individual sample estimates using ΔC* method from the Indian (Sabine *et al.*, 1999), Pacific (Sabine *et al.*, 2002), and Atlantic (Lee *et al.*, 2003) oceans were objectively gridded onto 33 depth surfaces with one degree resolution. These three sets of maps were merged with a fourth set of maps that was separately generated for the Southern Ocean. The mapped values were then vertically integrated to produce the vertical column inventory map shown in Figure 1 and summed to a global total inventory. Since the global survey had limited data coverage in the marginal basins (the South China Sea/Indonesian region, Yellow Sea, Japan/East Sea, Sea of Okhotsk, Gulf of Mexico, North Sea, Mediterranean Sea, and the Red Sea) and the Arctic Ocean (north of 65°N), these areas were excluded from the mapped regions. As shown in Figure 1, this anthropogenic CO_2 is not evenly distributed throughout the oceans.

The highest vertically integrated concentrations are found in the North Atlantic, leading this ocean basin to store 23% of the global oceanic anthropogenic CO_2, despite covering only 15% of the global ocean area. By contrast, the Southern Ocean south of 50°S has very low vertically integrated anthropogenic CO_2 concentrations, containing only 9% of the global inventory. More than 40% of the global inventory is found in the region between 50°S and 14°S because of the substantially higher vertically integrated concentrations and the large ocean area in these latitude bands (Fig. 1). Approximately 60% of the total anthropogenic CO_2 inventory is stored in the Southern Hemisphere, roughly in proportion to the larger ocean surface area of this hemisphere. The cumulative oceanic anthropogenic CO_2 sink for the period from 1800 to 1994, for the ocean region shown in Figure 1, is 106 ± 17 pg C. Accounting for the excluded regions, the estimated global anthropogenic CO_2 sink is 118 ± 19 pg C. The uncertainty in this total inventory is estimated from uncertainties in the anthropogenic CO_2 estimates and mapping errors.

Figure 2 shows the vertical distribution of anthropogenic CO_2 along representative meridion-

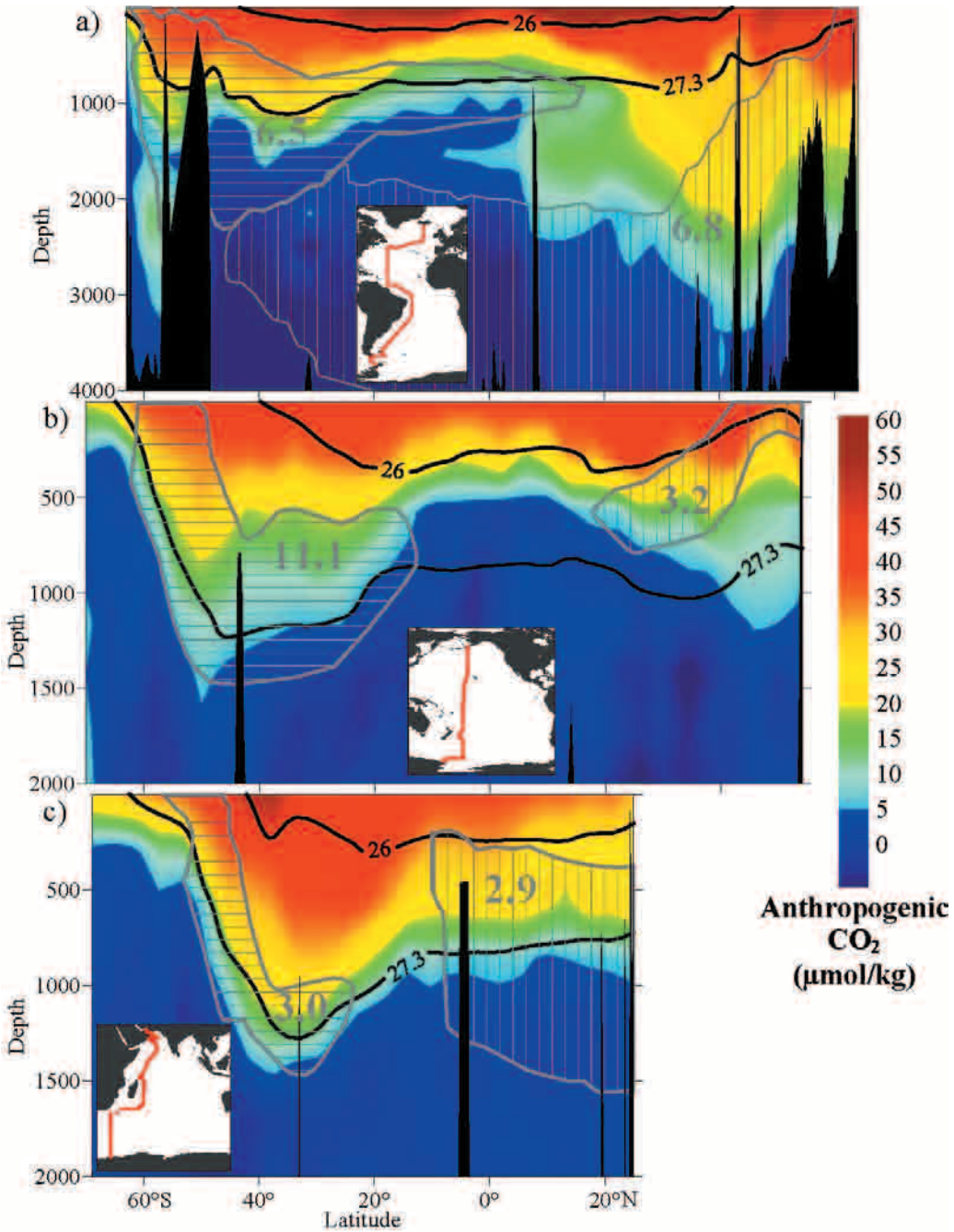

FIG. 2. – Sections of anthropogenic CO_2 (μmol kg^{-1}) from a) Atlantic, b) Pacific, and c) Indian Oceans. Gray hatched regions in the southern hemisphere in each ocean represent Antarctic Intermediate Water. Gray hatched regions in the northern hemisphere represent a) North Atlantic Deep Water, b) North Pacific Intermediate Water, and c) Red Sea /Persian Gulf Intermediate Water. The gray number is the total inventory (Pg C) within the hatched area. The bold lines are isopycnals with potential density values. Note that the depth scale for a) is twice that of the other panels, reflecting the deeper penetration in the North Atlantic. (Sabine *et al.*, 2004)

al sections in the Atlantic, Pacific and Indian oceans for the mid 1990s. The highest anthropogenic CO_2 concentrations are found in near-surface waters because anthropogenic CO_2 invades the ocean by gas exchange across the air-sea interface. Away from deep water formation regions, the mixing of near-surface waters downward into the deep ocean takes relatively long time. As a result, during the mid-1990's, the anthropogenic CO_2 concentration in most of the deep and abyssal ocean remained below the detection limit for the ΔC^* technique. According to Sabine *et al.* (2004), about 30% of the anthropogenic CO_2 is found shallower than 200 m and nearly 50% above 400 m depth. The global average depth of the 5 μmol kg^{-1} contour is approximately 1000 m. The majority of the

anthropogenic CO_2 in the ocean is, therefore, confined to the thermocline.

Variations in the penetration depth of anthropogenic CO_2 are determined by how rapidly the anthropogenic CO_2 that has accumulated in the near surface waters is transported into the interior of the ocean. This transport occurs primarily along isopycnal surfaces. These surfaces that are ventilated rapidly and those that are deflected deep into the interior of the ocean will lead to the deepest anthropogenic CO_2 penetration. The deepest penetrations are associated with convergence zones at temperate latitudes where water that has recently been in contact with the atmosphere can be transported into the ocean interior. The isopycnal layers in these regions tend to be thick and inclined, providing pathway for the movement of anthropogenic CO_2 laden waters into the ocean interior. Low vertical penetration is generally observed in regions of upwelling, such as the Equatorial Pacific, where intermediate-depth waters, low in anthropogenic CO_2, are transported toward the surface. The isopycnal layers in the tropical thermocline tend to be shallow and thin, minimizing the transport of anthropogenic CO_2 –laden waters into the ocean interior.

Figure 3a shows the distribution of anthropogenic CO_2 on a relatively shallow isopycnal surface with a potential density (σ_θ) of 26.0 (see depths in Fig. 2). About 20% of the anthropogenic CO_2 is stored in waters with potential densities equal to or less than that of this surface. The highest concentrations are generally found closest to where this density intersects the surface, an area referred to as the outcrop (e.g. heavy black line between 40°S and

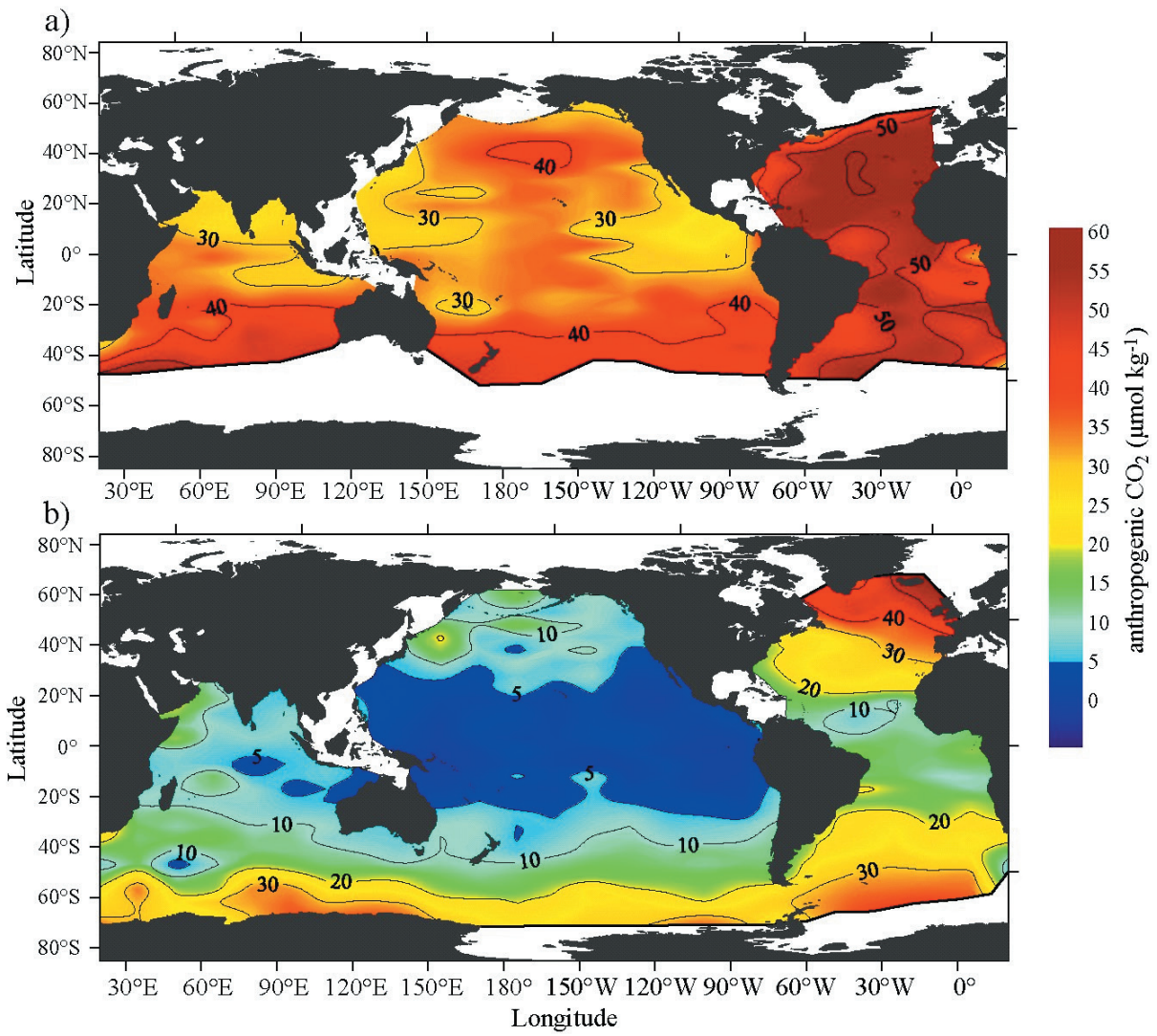

FIG. 3. – Maps of anthropogenic CO_2 on the potential density surface (a) σ_θ = 26.0 and (b) σ_θ = 27.3. Bold lines at the edge of the colored region indicate areas where the density surface outcrops. (Sabine *et al.*, 2004)

60°S in the fig.). Concentrations decrease away from these surface outcrops in the Indian and Pacific Oceans, primarily reflecting the aging of these waters, i.e. these waters were exposed to lower atmospheric CO_2 concentrations when they were last in contact with the atmosphere. The Atlantic waters do not show this trend because the 26.0 σ_θ surface is much shallower and therefore relatively well connected to the ventilated surface waters throughout most of the Atlantic (Fig. 2a, 3a).

The formation and transport of mode and intermediate waters is the primary mechanism for moving anthropogenic CO_2 to intermediate depths. The spatial distribution of anthropogenic CO_2 in these intermediate waters is illustrated with the 27.3 σ_θ surface (Fig. 3b), whose mean depth is about 900 m. As with the 26.0 σ_θ surface, anthropogenic CO_2 concentrations decrease away from the outcrop. On this deeper surface, however, slower ventilation results in stronger gradients and large areas where the anthropogenic CO_2 is below detection level. The Atlantic contains substantially higher anthropogenic CO_2 concentrations on the 27.3 σ_θ surface than the other basins, due in part to faster ventilation, but also because of the more favorable Revelle factor (see global distribution of Revelle factor in Fig. 3 of Sabine *et al.*, 2004). Although the formation of intermediate, mode, and deep waters provides the primary mechanism for moving anthropogenic CO_2 into the ocean interior, the magnitude and distribution of the anthropogenic signal can be quite different, depending on the nature of the water mass. As examples, some of the dominant intermediate water masses (i.e., North Atlantic Deep Water, North Pacific Intermediate Water, and Red Sea/Persian Gulf Intermediate Water in the northern hemisphere, and Antarctic Intermediate Water in the southern hemisphere) are outlined in Figure 2.

The subducted intermediate (for example, Antarctic Intermediate Water, i.e. AAIW) and mode waters, which contain high concentrations of anthropogenic CO_2, transported large amount of anthropogenic CO_2 into Southern Ocean. Together with the large volumetric contribution of water masses in Southern Hemisphere thermocline, the high anthropogenic CO_2 inventory, according to Sabine *et al.* (2004), is estimated to exceed 20 pg C in the Southern Ocean. About 3.2 pg C of anthropogenic carbon is found in the North Pacific Intermediate Water. Nearly 3 pg C can be found in the intermediate waters of the northern Indian Ocean. Globally, only 7% of the total anthropogenic CO_2 is found deeper than 1500 m. The only place where large concentrations of anthropogenic CO_2 penetrate to mid and abyssal depths is the North Atlantic because of the formation of Labrador Sea Water and North Atlantic Deep Water (NADW). In Sabine *et al.* (2004) calculations, nearly 7 pg of anthropogenic carbon is carried with NADW. Thus, NADW contains substantially less anthropogenic CO_2 than AAIW. There is little anthropogenic CO_2 associated with Antarctic Bottom Water. Because of the long mean residence time of deep water, the 1994 inventory estimated by Sabine *et al.* (2004) is only ~15% of the inventory it would have if the average surface anthropogenic CO_2 concentration of 56 μmol kg^{-1} were found throughout the ocean. This estimate does not account for the Revelle factor, which makes the CO_2 uptake capacity of the deep and intermediate waters much lower than that of the surface waters. Assuming an 80 ppm increase in global ocean pCO_2 values (equivalent to the 1994 atmospheric CO_2 increase from pre-industrial), the 1994 inventory would be ~30% of the global ocean potential at that time.

INCREASE OF ANTHROPOGENIC CO_2 IN THE OCEAN DURING THE PAST FEW DECADES

The anthropogenic CO_2 increase in the ocean with time can be estimated if separate survey data sets obtained at different times are available for analysis. The methods used to derive the estimates include the direct comparison of DIC on isopycnal surfaces of repeat surveys (Peng *et al.*, 1998) and the statistical analysis of data sets obtained at different times using Multi-parameter Linear Regression (MLR) method (Wallace, 1995; Peng *et al.* 2003).

Direct comparison of repeat surveys

Assuming an insignificant change in water masses during the repeat survey period, changes in DIC derived from a direct comparison reflect the anthropogenic CO_2 input over this time period. This idea has been explored by Peng *et al.* (1998) using repeat surveys in the Indian Ocean along 80° E from 20° S to 5° N. Six stations were occupied on this cruise line during the GEOSECS expedition in April 1978. During the NOAA/OACES I8NR cruise in 1995, sampling stations were occupied again along 80° E from 35° S to 5° N with a station spacing of 0.5 to 1 degree. Because no common references among these sets of measurements are available, data from

the two observational periods have to be converted to a common scale before the direct comparison can be made. Most of the water column below 2,000 m depth in this region of the Indian Ocean has had negligible contact with the atmosphere during the past 40 years, as suggested by the near absence of chlorofluorocarbons (Bullister, 1989). These waters respond very slowly on decadal timescales to changes in surface conditions. Hence, the chemical properties, such as DIC, Alk and dissolved O_2, should remain the same in deep water if there are no systematic errors between the cruises and if water masses remain the same. Results using this assumption of invariance of the properties of deep water show that Alk and O_2 are the same for both sets of measurements. However, all GEOSECS DIC values are systematically 21.3 ± 3.4 μmol kg^{-1} higher than those of the more recent I8NR cruise. Correction of such systematic shift in DIC has to be made first.

To minimize the influence of variations in thermocline depth over time, the DIC comparison is made along the same isopycnal surface. The observed properties are interpolated onto a few designated isopycnal surfaces. To avoid changes in the surface ocean caused mainly by seasonal variations, the isopycnal horizons in the upper thermocline are chosen. In the Indian Ocean, these waters are represented by potential density σ_θ values ranging from 26.6 to 27.2, which have a depth range of 300 to 1000 m. At these depths, the variations caused by the seasonal effect are expected to be minimal.

To reduce artifacts due to small natural variations in biological respiration between the two different periods, a correction is needed for the amount of DIC derived from respiration products. This is done by using the AOU data. The effect of changes in dissolution of $CaCO_3$ tests at two different times is corrected by using Alk data. To eliminate changes associated with variations in salinity, the corrected DIC is normalized to a salinity of 35.0 (as DIC_n).

Results of comparison show a significant increase in DIC from the GEOSECS survey to the new I8NR survey. The increases along the lighter isopycnals are greater than the denser isopycnals. The DIC concentrations are essentially indistinguishable from each other when the density reaches 27.2. In addition, the magnitude of changes is significantly larger in the latitude zone between 10° S and 20° S for all density horizons, indicating that more anthropogenic carbon is taken up in the temperate zone than in the equatorial zone during the period between the two surveys, which is consistent with bomb ^{14}C data (Broecker *et al*., 1995). Because T-S profiles do not indicate a significant change in water mass between the two surveys, the difference in DIC_n is assumed to represent the anthropogenic CO_2 signal. The mean difference of DIC between the two cruises on the same isopycnal surface is obtained by integrating the area between the two curves that represent the two surveys. The DIC increases range from 6 to 25 μmol kg^{-1} for the region between 20° S and 10° S, and 1 to 5 μmol kg^{-1} for the region between 10° S and 5° N. For the region as a whole, the 26.6 isopycnal has a DIC increase of the order of 12 μmol kg^{-1}, and this excess DIC decreases with the increasing density until no detectable signal at an isopycnal of 27.2. Based on the precision of DIC measurements from both cruises, and six repeat stations for comparison, the estimated random error for the mean difference is about ± 4.5 μmol kg^{-1}. Part of the reason for such high uncertainty is mainly that the GEOSECS data are less precise. In the future, better data can be compared with the high quality I8NR data as a baseline for detecting the increase in the CO_2 inventory over the next decade. Current estimates of accuracy of DIC are ± 1.5 μmol kg^{-1}, whereas the precision for Alk and O_2 is 2 and 0.2 μmol kg^{-1}, respectively, making detection of the anthropogenic CO_2 signal in the ocean over time more robust. Results from present CO_2/CLIVAR Repeat Hydrography Program could provide wealth of information on anthropogenic CO_2 increase since the WOCE/JGOFS surveys in the 1990s.

The rate of DIC increase during the time period between GEOSECS in 1978 and I8NR in 1995 is estimated to be 0.2 μmol kg^{-1} yr^{-1} (or 0.11 mol m^{-2} yr^{-1}) for the Indian equatorial region, and 1.1 μmol kg^{-1} yr^{-1} (or 0.65 mol m^{-2} yr^{-1}) for the Indian temperate region. The mean increase for the whole region is estimated to be 0.5 μmol kg^{-1} yr^{-1} (or 0.3 mol m^{-2} yr^{-1}). The total accumulated anthropogenic CO_2 for the whole width of Indian Ocean between 20°S and 5°N is estimated to be 1.64 pg C during this period. This is compatible with the Princeton model estimate of 1.47 pg C for the same area in this period (Murnane *et al*., 1999).

The increase of anthropogenic CO_2 in the Pacific Ocean over the last two decades was also estimated by this method for the northeastern region (Peng *et al*., 2003). The GEOSECS stations 201 to 214 occupied in 1974 are located on an east-west cruise line along 30°N latitude. A more recent NOAA/OACES CGC91 cruise in 1991 in this area ran north-south

along 152° W. Hence, the region where these two cruise lines crossed each other was selected for this direct comparison method. For CGC91, sampling stations within the latitude zone between 26°N and 34°N are selected. For GEOSECS, stations 202, 204, 212, and 213 with longitude between 140°W and 170°W are used. Isopycnal surfaces with σ_θ values 26.4, 26.6, 26.8, 27.0, 27.2 and 27.4, corresponding to upper thermocline, are selected for analysis. A linear interpolation method is used to derive the DIC and other related properties on these isopycnals from the nearest isopycnal surfaces where actual measurements were made. The DIC values from GEOSECS program are adjusted by -30.3 μmol kg^{-1} to eliminate the systematic offset in DIC measurements (see details next section under MLR method). Results of comparison of salinity normalized DIC between CGC91 and GEOSECS indicate that anthropogenic CO_2 has penetrated all the way into 27.4 isopycnal, which correspond to a depth of about 1120 m. At the shallower isopycnal of 26.4 (about 400 m), the anthropogenic CO_2 signal is about 19.4 ± 15.3 μmol kg^{-1}. The integrated total inventory of excess CO_2 added during the period 1974 to 1991 is estimated to be 16.0 ± 7.5 mol m^{-2}. The corresponding CO_2 uptake rate is 0.94 ± 0.44 mol m^{-2} yr^{-1}.

MLR method

The MLR method has been used to study the Indian Ocean ^{13}C Suess effect (Sonnerup *et al.*, 2000), and for estimating the change in anthropogenic CO_2 inventory in the Atlantic (Wallace, 1995), Indian (Sabine *et al.*, 1999) and Pacific Oceans (Slansky *et al.*, 1997; Peng *et al.*, 2003). The direct comparison of two sets of DIC measurements made at different times to determine the temporal changes in carbon inventories is subject to uncertainties caused by (1) spatial variability of DIC due to movement of water mass and (2) temporal variability of DIC in a water mass resulting from changes due to water mass mixing and/or changes in the rate of remineralization of organic and inorganic matter in the water mass. To compensate for these factors in order to reduce the uncertainties, an analysis using Multiple-parameter Linear Regression (MLR) method was suggested by Wallace (1995). In this method, a statistical model is used to determine the coefficients that describe the variations of carbon in the ocean as a function of various other properties. To detect the net changes of DIC due to the uptake of anthropogenic CO_2, it is assumed that the processes of anthropogenic CO_2 accumulation are not directly related to biological activities, and the relationship between DIC and other properties of water mass such as temperature, salinity, oxygen and nutrient concentrations remains unchanged in the time period of interest except for the DIC increase caused by invasion of anthropogenically produced CO_2.

Taking the Pacific Ocean as an example, the NOAA Climate and Global Change (CGC) cruises CGC91 and CGC96 are chosen for analysis. These two cruises cover the meridional transects in the North and South Pacific Ocean in 1991 and 1996, respectively. These datasets are compared with the observations collected during the GEOSECS program in 1973-74. Before the analysis of changes in DIC from GEOSECS to recent WOCE/JGOFS cruises, it is needed to verify if data collected at these two periods are compatible with each other without any systematic errors. To determine if systematic deviations exist, comparisons of data obtained in water samples deeper than 1500 m are made between GEOSECS survey (1973-74) and all the WOCE/WHP cruises in the Pacific (1990s). These comparisons are made for GEOSECS and WOCE stations that are within two degrees of latitude or longitude of each other. The assumption is made that deep water properties in these crossover stations should remain the same even though measurements were made about two decades apart because water masses at these depth are free of anthropogenic and other short term natural variability. Hydrographic properties, such as temperature, salinity, and oxygen, silicate, nitrate, and phosphate concentration, are chosen for comparison along with the carbon chemistry parameters DIC and Alk. Comparison of hydrographic properties at these crossover stations shows that the old and new data are highly consistent. To estimate the difference of these hydrographic properties measured during the two different time periods, the deep isopycnal method (Lamb *et al.* 2002) is applied using σ_4 isopycnal surface from 45.5 to 46.0 (approximate depth ranges from 1500 to 4500 m) for the comparison. The mean difference of salinity (GEOSECS – WOCE) for all crossover stations is –0.0016 ± 0.0020, and the mean potential temperature difference is –0.0072 ± 0.0069°C. These are considered as basin-wide mean offsets which are not significant enough to cause extra uncertainty in MLR calculations. Comparison of oxygen and nutrient concen-

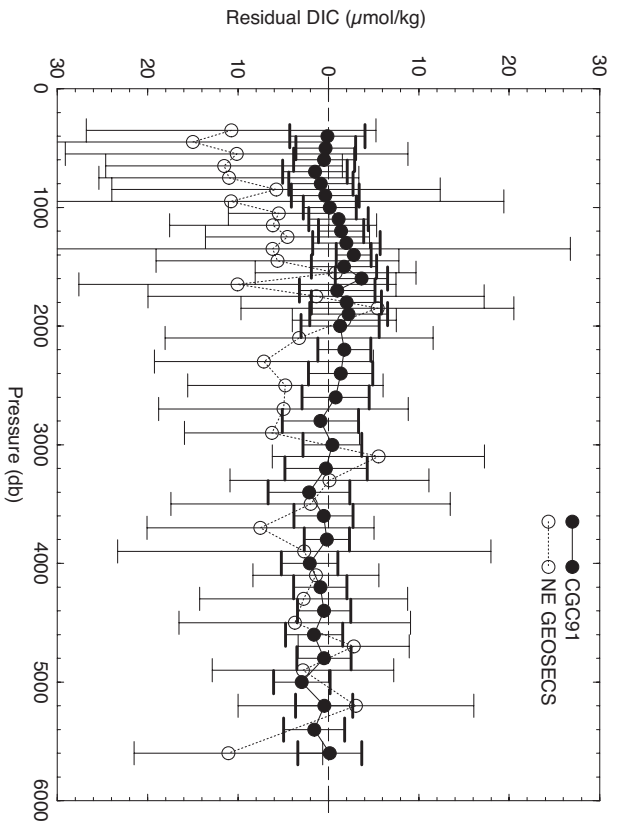

FIG. 4. – The distribution of residual DIC after all samples are binned into 100 m layers over the upper 2000 m depth and into 200 m layers below 2000 m depth. The solid circles with heavy error bars are from CGC91, open circles with lighter error bars are from GEOSECS stations in the Northeastern Pacific.

trations gives the basin-wide mean offsets as follows: O_2 concentration of –0.2 ± 5.0 μmol kg^{-1} , silicate difference of 2.6 ± 1.2 μmol kg^{-1}, NO_3 difference of 0.3 ± 1.0 μmol kg^{-1} , and PO_4 difference of –0.06 ± 0.03 μmol kg^{-1}. These results suggest that hydrographic properties are consistent for old and new data sets. However, DIC data in GEOSECS show systematically and consistently higher values than recent data set, giving a basin-wide mean DIC difference of 27.9 ± 9.1 μmol kg^{-1}. The GEOSECS Alk values are also consistently higher but with significant degree of scatter, showing a mean Alk difference of 11.1 ± 15.2 μmol kg^{-1}.

The offsets can also be derived from the MLR method. A relationship between DIC and these hydrographic properties from the recent data set at each crossover station is derived. This linear equation can be given as: $DIC = a + b\cdot\theta + c\cdot S + d\cdot O_2$, where θ is potential temperature, S is salinity, a, b, c, and d are constants determined using the recent data. The MLR results show that R^2 values for DIC linear regression of the recent data are better than 0.97. The assumption is made that this relationship remains the same in deep water over a time period of about two decades between GEOSECS and WOCE in each particular crossover location. This equation and derived coefficients are then used to compute the expected DIC at GEOSECS time using ζ, S, and O_2 values of GEOSECS dataset at the crossover station. The difference between the observed DIC and the computed DIC is considered as the estimated offset. The mean offset for a single GEOSECS crossover station is computed from samples below 2000 m depth, and the standard deviation from the mean is computed from these offsets. The mean Alk offsets between GEOSECS and WOCE are also computed in the same way, namely using the equation $Alk = a + b\cdot\theta + c\cdot S + d\cdot O_2$ where a, b, c, and d are constants determined separately for each crossover station using MLR method. Results show that the mean offsets for DIC values observed at GEOSECS time are consistently higher than recent data by 30.3 ± 7.0 μmol kg^{-1}, while the Alk values also show consistently higher values with a mean of 18.6 ± 7.1 μmol kg^{-1}. These results are slightly higher than those derived from deep isopycnal method, but basically they are consistent within the estimated uncertainty. Takahashi *et al*. (1985) reported the corrections for GEOSECS DIC and Alk data. Although they did not specifically mention the corrections for Pacific data, their analysis of Atlantic and Indian Oceans data implied that the Pacific data need a correction of –29 ± 8 μmol kg^{-1} for DIC, and –14 ± 4 μmol kg^{-1} for Alk. These results are consistent with the current estimates. For the analysis of anthropogenic CO_2 increase, we applied the correction obtained from the MLR method of -30.3 μmol kg^{-1} for all DIC and -18.6 μmol kg^{-1} for all Alk samples obtained for GEOSECS.

Analysis of 802 observations made during the CGC91 in the NE Pacific using the MLR method by assuming DIC as a function of 5 independent variables (AOU, θ, S, Si, and PO_4), the multiple R^2 = 0.997 is obtained. The standard error of residuals (observed minus fitted DIC) is estimated to be 3.6 μmol kg^{-1}. The distribution of residual DIC for all samples is binned into 100 m layers over the upper 2000 m depth and into 200 m layers below 2000 m (Fig. 4). These mean residuals meander along the zero residual line with depth. These residuals are compared with those derived from GEOSECS data using the same DIC function derived from CGC91. Before comparing the predicted DIC with the observed values, a correction of -30.3 μmol kg^{-1} is made to all the GEOSECS DIC samples because of

systematic DIC offset described earlier. The GEOSECS residual DIC (i.e., corrected DIC minus predicted DIC) represents the deviation of the observed DIC in 1973 from the expected DIC if measurement was made in 1991. Hence, any increase in DIC from 1973 to 1991 results in negative residual in DIC for the GEOSECS data. As we can see in Figure 4, the similarly binned GEOSECS residual DIC values are consistent with that derived from CGC91 for water below about 1500m. However, the water above 1500m shows negative residuals, indicating that DIC observed during the GEOSECS program 17 years before contained less DIC than the recent survey. The increase in DIC computed using atmospheric pCO_2 increase of 25.4 μatm during this period is ~16.3 μmol kg^{-1}. The increase in DIC during the same period as estimated from this MLR method reaches as high as 15 μmol kg^{-1}. However, the GEOSECS residual DIC suffers from a high standard deviation, which overlaps with CGC91 residual DIC. This is mainly due to the quality of the DIC data obtained during the GEOSECS program. The overall precision of DIC measurement has been estimated to be ±11 μmol kg^{-1} (Takahashi, 1983). The standard deviation of correction for systematic offset is ±9 μmol kg^{-1}. The propagation of these errors leads to an uncertainty of ±14 μmol kg^{-1}. Based on comparison of CGC91 with GEOSECS in the NE Pacific data between 300 and 600 m depth, we obtain a mean increase in anthropogenic CO_2 concentration of 11.9 ± 20.5 μmol kg^{-1} for the upper 600 m of water column. The integrated water column anthropogenic CO_2 inventory is estimated to be 21.3 ± 7.9 mol m^{-2}. This increase in CO_2 inventory gives the mean anthropogenic CO_2 uptake rate over 17 years of 1.3 ± 0.5 mol m^{-2} yr^{-1}. This is compatible with 0.94 ± 0.44 mol m^{-2} yr^{-1} derived for the northeastern Pacific region using direct comparison along isopycnal surfaces of repeat surveys (Peng *et al.*, 2003).

Regression of 1170 observations obtained during CGC96 in the region north of 50°S in the South Pacific using the MLR method by assuming DIC as a function of five independent variables (AOU, θ, S, Si, and PO_4) gives a multiple $R^2 = 0.995$ and a DIC residual standard error of 4.3 μmol kg^{-1}. To quantify the anthropogenic CO_2 signal since the GEOSECS time in 1974, all GEOSECS stations in the South Pacific between 180° and 120° W are selected for determining the DIC residuals. After correction for a systematic DIC offset of 30.3 μmol kg^{-1} from the GEOSECS data, the binned residuals are shown in Figure 5. The penetration of anthropogenic CO_2

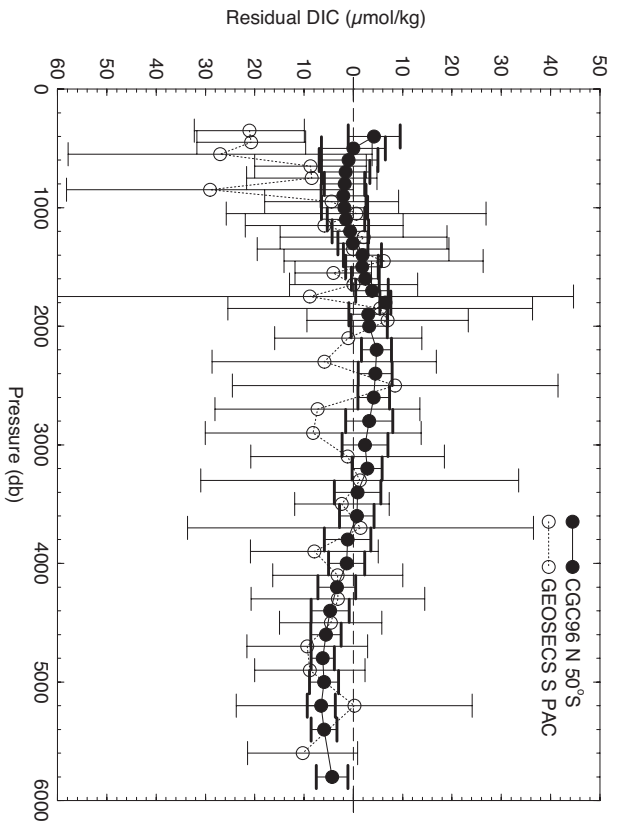

FIG. 5. – The distribution of residual DIC after all samples are binned into 100 m layer over the upper 2000 m depth and into 200 m layer below 2000 m depth. The solid cicles with heavy error bars are from CGC96, and open circles with lighter error bars are from GEOSECS in the South Pacific for stations north of 50°S between 120°W and 180° longitudes.

above 1000 m is clearly shown. The expected increase in DIC for the surface water is estimated to be 20.2 μmol kg^{-1}. The observed mean DIC residual of GEOSECS is estimated from the measurements between 300 and 500 m to be about 20.9 ± 15.7 μmol kg^{-1}. The water column integrated anthropogenic CO_2 inventory from surface water to 1000 m depth for the time period between 1974 and 1996 is estimated to be 19.7 ± 5.7 mol m^{-2}. The mean uptake rate of anthropogenic CO_2 in 22 years is estimated to be about 0.9 ± 0.3 mol m^{-2} yr^{-1}.

Combined with ΔC* method, Sabine *et al.* (1999) applied MLR method to evaluate excess CO_2 in the Indian Ocean from GEOSECS data collected in 1978 to WOCE data in 1995. This same method is being used for evaluating the increase of anthropogenic CO_2 in the Atlantic Ocean since GEOSECS time in 1973 (Peng and Wanninkhof, in preparation). Based on data set of 12 cruises carried out in the Eastern North Atlantic Ocean from 1977 to 1997, Rios *et al.* (2001) reported a time series of total anthropogenic CO_2 inventories during this period. An average rate of

TABLE 1. – Summary of rates of anthropogenic CO_2 uptake by ocean in past few decades.

Area of study	Years of obs.	CO_2 uptake rate (mol m^{-2} yr^{-1})	Method	Reference
Indian along 80°E	1978-1995		Isopycnal	Peng *et al*., 1998
Equatorial region		0.11		
South Temperate		0.65		
NE Pacific	1974-1991	0.94 ± 0.44	Isopycnal	Peng *et al*., 2003
NE Pacific	1974-1991	1.3 ± 0.5	MLR	Peng *et al*., 2003
S Pacific	1974-1996	0.9 ± 0.3	MLR	Peng *et al*., 2003
NE Atlantic	1977-1997	0.95	Inventory	Rios *et al*., 2001

anthropogenic CO_2 uptake of 0.95 mol m^{-2} yr^{-1} was derived from the rate of change of the integrated anthropogenic CO_2 down to 2000 m depth. This result is consistent with rates of CO_2 uptake discussed in this section. Table 1 summarizes the rate of anthropogenic CO_2 uptake in the global oceans.

IMPACT OF OCEANIC ANTHROPOGENIC CO_2 ON THE OCEAN CHEMISTRY

The impact of anthropogenic CO_2 on the calcium carbonate system in the oceans has been discussed extensively (Feely *et al*., 2004). Estimates of future atmospheric and oceanic CO_2 concentrations suggest that by the end of the century atmospheric CO_2 levels could be over 800 ppm (Albritton and Meira Filho, 2001). Corresponding ocean models predict that surface water DIC could probably increase by more than 12%, and the carbonate ion concentration would decrease by 60% (Brewer, 1997). The corresponding effect on surface waters would be a drop of about 0.4 pH units (Caldeira and Wickett, 2003). Such dramatic changes of the carbon system in open ocean surface waters have probably not occurred for the past few millions of years. If these chemical changes do occur in the future, they can potentially have significant impacts on the biological systems in the oceans as well.

Processes that increase the Alk in the upper ocean facilitate the uptake of anthropogenic CO_2 from the atmosphere. The dissolution of marine carbonates, including biogenic magnesium calcite (from coralline algae), aragonite (from corals and pteropods), and calcite (from coccolithophorids and foraminifera) neutralizes anthropogenic CO_2 and adds to Alk by the chemical reaction:

$$CO_2 + CaCO_3 + H_2O \rightarrow 2HCO_3^- + Ca^{2+}$$

The carbonate shells of marine plankton produced in the euphotic zone play a major role in this reaction. Upon death of plankton, their carbonate shells fall through the water column and are either dissolved or deposited in shallow or deep-sea sediments. As oceans become enriched in anthropogenic CO_2, the locations of dissolution will change and the extent of dissolution will increase as a function of the decrease in the $CaCO_3$ saturation state. The general understanding is that the dissolution of pelagic $CaCO_3$ particles primarily occurs at great depths below the calcite saturation horizon (Broecker and Peng, 1982). However, recent analyses of the global carbonate budget and carbonate data for the global oceans (Milliman, 1993; Milliman, *et al*., 1999) have indicated that perhaps as much as 60 to 80% of the $CaCO_3$ that is exported out of surface ocean dissolves in the upper 1000 m. Extensive studies of $CaCO_3$ dissolution as a result of increasing anthropogenic CO_2 in the ocean using recent WOCE/JGOFS global carbon survey data have resulted in a number of publications, including Feely at al. (2004) for the global oceans, Feely *et al*.(2002) for the Pacific Ocean, Chung *et al*., (2003 and 2004) for the Atlantic Ocean. Feely *et al*. (2004) reported that a comparison of the pre-industrial and present day $CaCO_3$ saturation horizons reveals several distinct regions where the undersaturation zone has expanded. In regions between 20°N and 50°N in the North Atlantic Ocean, the aragonite saturation horizon for the pre-industrial era is nearly the same as today. In the eastern South and North Atlantic, however, the aragonite saturation horizon has migrated upward by about 80 to 150 m between 50°S and 15°N. In the Indian Ocean, saturation depths have shoaled increasingly north of 30°S, so that aragonite saturation depths in the Arabian Sea and Bay of Bengal are now 100 to 200 m shallower than in pre-industrial times. In the Pacific, the upward migration of the aragonite saturation horizon is between 30 and 80 m south of 38°S and between 30 and 100 m north of 3°N. The calcite saturation horizon has also shoaled by about 40 to 100 m north of 20°N in the North Pacific. Such shoaling

is due to the effects of anthropogenic CO_2 ventilation and biological respiration processes in the intermediate waters. This implies that the dissolution of $CaCO_3$ particles will likely increase as the waters become increasingly undersaturated over time due to increasing anthropogenic CO_2 uptake.

REFERENCES

Albritton, D.L. and L.G. Meira Filho. – 2001. The scientific basis: Technical summary. In: R.T. Watson, (eds.), *Climate Change 2001 Synthesis Report: Contribution of Working Group I to the Third Assessment Report of the Intergovernmental Panel on Climate Change,* pp. 167–218. Cambridge Univ. Press. New York.

Anderson, L.A. and J.L. Sarmiento. – 1994. Redfield ratios of remineralization determined by nutrient data analysis, *Global Biogeochem. Cycles*, 8, 65-80.

Brewer, P.G. – 1978. Direct measurement of the oceanic CO_2 increase., *Geophys. Res. Lett.,* 5: 997-1000.

Brewer, P.G. – 1997. Ocean chemistry of the fossil fuel CO_2 signal: The haline signature of "Business as Usual". *Geophys. Res. Lett.,* 24: 1367-1369.

Broecker, W.S. and T.-H. Peng.-1982. *Tracers in the Sea*. Lamont-Doherty Geological Observatory of Columbia University, Palisades, New York.

Broecker, W.S., T. Takahashi and T.-H. Peng. – 1985. Reconstruction of past atmospheric CO_2 contents from the chemistry of the contemporary ocean. U.S. Dept. of Energy, Report DOE/OR-857.

Broecker, W.S., S. Sutherland, W. Smethie, T.-H. Peng, and G. Ostlund. – 1995. Oceanic radiocarbon: Separation of the natural and bomb components. *Global Biogeochem. Cycles,* 9, 263-288.

Bullister, J.L. – 1989. Chlorofluorocarbons as time dependent tracers in the ocean. *Ocean Mag.,* 2: 12-17.

Caldeira, K. and M.E. Wickett. – 2003. Anthropogenic carbon and ocean pH. *Nature,* 425: 325-325.

Chen, C.-T. and F.J. Millero. – 1979. Gradual increase of oceanic CO_2. *Nature*, 277: 205-206.

Chung, S.-N., K. Lee, R.A. Feely, C.L. Sabine, F.J. Millero, R. Wanninkhof, J.L. Bullister, R.M. Key and T.-H. Peng. – 2003. Calcium carbonate budget in the Atlantic Ocean based on water column inorganic carbon chemistry. *Global Biogeochem. Cycles,* 17, 1093, doi:10.1029/2002GB002001.

Chung, S.-N., G.-H. Park, K. Lee, R.M. Key, F.J. Millero, R.A. Feely, C.L. Sabine, P.G. Falkowski. – 2004. Postindustrial enhancement of aragonite undersaturation in the upper tropical and subtropical Atlantic Ocean: The role of fossil fuel CO_2. *Limnol. Oceanogr.,* 49: 315-321.

Feely, R.A., C.L. Sabine, K. Lee, F.J. Millero, M.F. Lamb, D. Greeley, J.L. Bullister, R.M. Key, T.-H. Peng, A. Kozyr, T. Ono and C.S. Wong. – 2002. In situ calcium carbonate dissolution in the Pacific Ocean. *Global Biogeochem. Cycles* 16, 1144.

Feely, R.A., C.L. Sabine, K. Lee, W. Berelson, J. Kleypas, V.J. Fabry and F.J. Millero. – 2004. Impact of anthropogenic CO_2 on the $CaCO_3$ system in the oceans. *Science*, 305: 362-366.

Gruber, N., J.L. Sarmiento and T.F. Stocker. – 1996. An improved method for detecting anthropogenic CO_2 in the oceans. *Global Biogeochem. Cycles*, 10: 809-837.

Keeling, C.D. and T.P. Whorf. – 1994. Atmospheric CO_2 records from sites in the SIO air sampling network. In: Boden *et al.*, (eds.), *Trends '93: A Compendium of Data on Global Change*, TRep. ORNL/CDIAC-65, pp. 16-26, CDIAC, Oak Ridge Nat. Lab., Oak Ridge, Tenn.

Lamb, M.F., C.L. Sabine, R.A. Feely, R. Wanninkhof, R.M. Key, G.C. Johnson, F.J. Millero, K. Lee, T.-H. Peng, A. Kozyr, J.L. Bullister, D. Greeley, R.H. Byrne, D .W. Chipman, A.G. Dickson, C. Goyet, P.R. Guenther, M. Ishii, K.M. Johnson, C.D. Keeling, T. Ono, K. Shitashima, B. Tilbrook, T. Takahashi, D.W.R. Wallace, Y.W. Watanabe, C. Winn and C.S. Wong. – 2002: Consistency and synthesis of Pacific Ocean CO2 survey data. *Deep-Sea Res. II*, 49: 21-58.

Lee, K., S.-D. Choi, G.-H. Park, R. Wanninkhof, T.-H. Peng, R.M. Key, C.L. Sabine, R.A. Feely, J.L. Bullister, F.J. Millero, and A. Kozyr. – 2003. An updated anthropogenic CO_2 inventory in the Atlantic Ocean. *Global Biogeochem. Cycles*, 17, 1116, doi:10.1029/2003GB002067.

Milliman, J.D. – 1993. Production and accumulation of calcium carbonate in the ocean: Budget of a nonsteady state. *Global Biogeochem. Cycles,* 7: 927-957.

Milliman, J.D., P.J. Troy, W.M. Balch, A.K. Adams and Y.-H. Li, and F.T. Mackenzie. – 1999. Biologically mediated dissolution of calcium carbonate above the chemical lysocline. *Deep-Sea Res. I,.* 46: 1653-1669.

Murnane, R.J., J.L. Sarmiento, and C. LeQuéré. – 1999: Spatial distribution of air-sea CO2 fluxes and the interhemispheric transport of carbon by the oceans. *Global Biogeochem.Cycles*, 13(2): 287-305.

Neftel, A., H. Friedli, E. Moor, H. Lotscher, H. Oeschger, U. Siegenthaler, and B. Stauffer. – 1994. Historical CO_2 record from the Siple station ice core. In: T. Boden *et al.* (eds.), *Trends '93: A Compendium of Data on Global Change*. Rep. ORNL/CDIAC-65, pp. 11-14, CDIAC, Oak Ridge Nat. Lab., Oak Ridge, Tenn.

Peng, T.-H., R. Wanninkhof, J. Bullister, R. Feely and T. Takahashi. – 1998. Quantification of decadal anthropogenic CO2 uptake in the Ocean based on dissolved inorganic carbon measurements. *Nature*, 396: 560-563.

Peng, T.-H., R. Wanninkhof and R. A. Feely. – 2003. Increase of anthropogenic CO_2 in the Pacific Ocean over the last two decades. *Deep-Sea Res. II,* 50: 3065-3082.

Perez, F.F., M. Alvarez, and A.F. Rios. – 2002. Improvements on the back-calculation technique for estimating anthropogenic CO_2. *Deep Sea Res. I*, 49: 859-875.

Rios, A.F., F.F. Perez and F. Fraga. – 2001. Long-term (1977-1997) measurements of carbon dioxide in the Eastern North Atlantic: evaluation of anthropogenic input. *Deep Sea Res. II*, 48: 2227-2239.

Sabine, C.L., R.M. Key, K.M. Johnson, F.J. Millero, A. Poisson, J.L. Sarmiento, D.W.R. Wallace and C.D. Winn. – 1999. Anthropogenic CO_2 inventory of the Indian Ocean. *Global Biogeochem. Cycles*, 13: 179-198.

Sabine, C.L., R.A. Feely, R.M. Key, J.L. Bullister, F.J. Millero, K. Lee, T.-H. Peng, B. Tilbrook, T. Ono and C.S. Wong. – 2002. Distribution of anthropogenic CO_2 in the Pacific Ocean. *Global Biogeochem. Cycles*, 16, 1083, doi: 10.1029/2001GB 001639.

Sabine, C.L., R.A. Feely, N. Gruber, R.M. Key, K. Lee , J.L. Bullister, R. Wanninkhof, C.S. Wong, D. W.R. Wallace, B. Tilbrook, F.J. Millero, T.-H. Peng, A. Kozyr, T. Ono and A. F. Rios. – 2004. The oceanic sink for anthropogenic CO_2. *Science*, 305: 367-371.

Shiller, A.M. – 1981. Calculating the oceanic CO_2 increase: a need for caution. *J. Geophys. Res.*, 86: 11083-11088.

Shiller, A.M. – 1982. Reply to "Comment on calculating the oceanic CO_2 increase: a need for caution, by A.M. Shiller". *J. Geophys. Res.*, 87: 2086.

Slansky, C.M., R.A Feely and R. Wanninkhof. – 1997. The stepwise linear regression method for calculating anthropogenic CO_2 invasion into the north Pacific Ocean. In: S. Tsunogai (ed.), *Biogeochemical Processes in the North Pacific, Proceedings of the International Marine Science Symposium on Biogeochemical Processes in the North Pacific*, pp. 70-79. Mutsu, Japan, Japan Marine Science Foundation.

Sonnerup, R.E., P.D. Quay and A.P. McNichol. – 2000. The Indian Ocean ^{13}C Suess effect, *Global Biogeochem. Cycles*, 14: 903-916.

Takahashi, T. – 1983. Precision of the alkalinity and total CO_2 measurements. In: R. Weiss, W.S. Broecker, H. Craig and D. Spencer (eds.), *GEOSECS Indian Ocean Expedition* Vol. 5. pp. 5-7. U.S. Gov. Printing Office, Washington D.C.

Takahashi, T., W.S. Broecker and S. Langer. – 1985. Redfield ratio based on chemical data from isopycnal surfaces. *J. Geophys. Res.*, 90: 6907-6924.

Wallace, D.W.R. – 1995. Monitoring global ocean carbon inventories. Ocean Observing System Development Panel, Texas A and M University, College Station, TX, 54 pp.